



1    **Blowing Snow Sublimation and Transport over Antarctica from 11 Years of CALIPSO**

2    **Observations**

3    Stephen P Palm<sup>1</sup>, Vinay Kayetha<sup>1</sup>, Yuekui Yang<sup>2</sup> and Rebecca Pauly<sup>1</sup>

4    <sup>1</sup>Science Systems Applications Inc., 10210 Greenbelt Road, Greenbelt, Maryland USA 20771.

5    <sup>2</sup>NASA Goddard Space Flight Center, Greenbelt, Maryland USA 20771.

6

7    Address for all correspondence:

8    Stephen Palm, Code 612, NASA Goddard Space Flight Center, Greenbelt, Maryland USA 20771.

9    Email: stephen.p.palm@nasa.gov

10   Phone: +1-301-614-6276

11

12   **ABSTRACT**

13   Blowing snow processes commonly occur over the earth's ice sheets when near surface wind  
14   speed exceeds a threshold value. These processes play a key role in the sublimation and re-  
15   distribution of snow thereby influencing the surface mass balance. Prior field studies and  
16   modeling results have shown the importance of blowing snow sublimation and transport on the  
17   surface mass budget and hydrological cycle of high latitude regions. For the first time, we  
18   present continent-wide estimates of blowing snow sublimation and transport over Antarctica  
19   based on direct observation of blowing snow events. We use an improved version of the  
20   blowing snow detection algorithm developed for previous work that uses atmospheric  
21   backscatter measurements obtained from the CALIOP lidar aboard the CALIPSO satellite. The  
22   blowing snow events identified by CALIPSO and meteorological fields from MERRA-2 are used  
23   to compute the sublimation and transport rates. Our results show that maximum sublimation  
24   occurs along and slightly inland of the coastline. This is contrary to the observed maximum  
25   blowing snow frequency which occurs over the interior. The associated temperature and  
26   moisture re-analysis fields likely contribute to the spatial distribution of the maximum  
27   sublimation values. However, the spatial pattern of the sublimation rate over Antarctica is  
28   consistent with modeling studies and precipitation estimates. Overall, our results show that  
29   Antarctica average integrated blowing snow sublimation is about  $393.4 \pm 138 \text{ Gt yr}^{-1}$  which is



30 considerably larger than previous model-derived estimates. We find maximum blowing snow  
31 transport amount of 5 Megatons  $\text{km}^{-1} \text{ yr}^{-1}$  over parts of East Antarctica and estimate that the  
32 average snow transport from continent to ocean is about  $3.68 \text{ Gt yr}^{-1}$ . These continent-wide  
33 estimates are the first of their kind and can be used to help model and constrain the surface-  
34 mass budget over Antarctica.

35

36 **Keywords:** Blowing snow, sublimation, transport, CALIPSO, Antarctica, surface mass balance

37

## 38 1 Introduction

39 The surface mass balance of the earth's great ice sheets that cover Antarctica and Greenland is  
40 one of today's most important topics in climate science. The processes that contribute to the  
41 mass balance of a snow or ice-covered surface are precipitation, surface runoff (melting),  
42 removal/loss (erosion/sublimation) and deposition of snow mass (wind transport). Sublimation  
43 of snow can occur at the surface but is greatly enhanced within the atmospheric column of the  
44 blowing snow layer. The contributions of these processes to the mass balance vary greatly  
45 spatially, and can be highly localized and very difficult to quantify.

46 It is well known that the Arctic is experiencing rapid warming and loss of sea ice cover and  
47 thickness. In the past few decades, the Arctic has seen an increase in average surface air  
48 temperature by  $2 \text{ }^{\circ}\text{C}$  (Przybylak, 2007). Modeling studies suggests an increase in annual mean  
49 temperatures over the Arctic by  $8.5 \pm 4.1 \text{ }^{\circ}\text{C}$  over the current century that could lead to a  
50 decrease in sea ice cover by  $49 \pm 18 \text{ \%}$  (Bintanja and Krikken, 2016). While the Antarctic has  
51 experienced an increase in average surface temperature, most of the warming is observed over  
52 West Antarctica at a rate of  $0.17 \text{ }^{\circ}\text{C}$  per decade from 1957 to 2006 (Steig et al., 2009; Bromwich  
53 et al., 2013). Such surface warming undoubtedly has implications for ice sheet mass balance  
54 and sea level rise mainly through the melting term of the mass balance equation. However, the  
55 other processes affecting the mass balance of ice sheets may also be experiencing changes that  
56 are difficult to identify and quantify. For instance, models have shown that in a warming  
57 climate, precipitation should increase over Antarctica and most of it will fall as snow (Church et



58 al., 2013). If snowfall is increasing, perhaps the frequency of blowing snow and subsequently  
59 the magnitude of transport and sublimation will increase as well. Thus, understanding how  
60 these processes affect the overall mass balance of the ice sheets and how they may be  
61 responding to a changing climate, is of growing concern.

62 In addition to ice sheet mass balance, sublimation of blowing snow is also important for the  
63 atmospheric moisture budget in high latitudes. For instance, in the Canadian Prairies and parts  
64 of Alaska sublimation of blowing snow was shown to be equal to 30 % of annual snowfall  
65 (Pomeroy et al., 1997). About 50 % of the wind-transported snow sublimates in the high plains  
66 of southeastern Wyoming (Tabler et al., 1990). Adequate model representation of sublimation  
67 processes are important to obtain reliable prediction of spring runoff and determine the spatial  
68 distribution/variability of energy and water fluxes and their subsequent influence on  
69 atmospheric circulation in high latitude regions (Bowling et al., 2004).

70 Over Antarctica, blowing snow occurs more frequently than anywhere else on earth. Models  
71 driven by long-term surface observations over the Neumayer station (East Antarctica), estimate  
72 that blowing snow sublimation removes up to 19 % of the solid precipitation (Van den Broeke  
73 et al., 2010). Over certain parts of the Antarctica, where persistent katabatic winds prevail,  
74 blowing snow sublimation is found to remove up to 85 % of the solid precipitation (Frezzotti et  
75 al., 2002). Over coastal areas up to 35% of the precipitation may be removed by wind through  
76 transport and sublimation (Bromwich 1988). Das et al., (2013) concluded that ~ 2.7–6.6 % of  
77 the surface area of Antarctica has persistent negative net accumulation due to wind scour  
78 (erosion and sublimation of snow). These studies show the potential role of the blowing snow  
79 sublimation process in the surface mass balance of the earth's ice sheets.

80 For the current work, we focus on blowing snow processes over the Antarctic region. Due to the  
81 uninhabited expanse of Antarctica and the lack of observations, prior, continent-wide studies of  
82 blowing snow sublimation over Antarctica had to rely on parameterized methods that use  
83 model re-analysis of wind speed and low level moisture. The presence of blowing snow is  
84 inferred from surface temperature, wind speed and snow age (if known). In a series of papers  
85 on the modeling of blowing snow, Dery and Yau (1998, 1999, 2001) develop and test a  
86 parameterization of blowing snow sublimation. Their results show that most sublimation occurs



87 along the coasts and over sea ice with maximums in some coastal areas of 150 mm snow water  
88 equivalent (swe). Lenearts et al., (2012a) utilized a high resolution regional climate model  
89 (RACMO2) to simulate the surface mass balance of the Antarctic ice sheet. They found drifting  
90 and blowing snow sublimation to be the most significant ablation term reaching values as high  
91 as 200 mm  $\text{yr}^{-1}$  swe along the coast. There has been some work done on blowing snow  
92 sublimation from field measurements, but the data are sparse and measurements are only  
93 available within the surface layer (< 10 m). For instance, average monthly rates of sublimation  
94 calculated for Halley Station, Antarctica, varied between 0.13 to 0.44 mm day $^{-1}$  (King et al.  
95 2001).

96 While transport of blowing snow is considered to be less important than sublimation in terms  
97 of mass balance of the Antarctic ice sheet, erosion and transport of snow by wind can be  
98 considerable in certain regions. Das et al., (2013) have shown that blue ice areas are frequently  
99 seen in Antarctica. These regions exhibit a negative mass balance as all precipitation that falls is  
100 either blown off or sublimated away. Along the coastal regions it has been argued that  
101 considerable mass is transported off the coast via blowing snow in preferential areas dictated  
102 by topography (Scarchilli et al., 2010). In the Tera Nova Bay region of East Antarctica, manned  
103 surface observations show that drifting and blowing snow occurred 80 % of the time in fall and  
104 winter and cumulative snow transport was 4 orders about of magnitude higher than snow  
105 precipitation. Much of this airborne snow is transported off the continent producing areas of  
106 blue ice. Such observations raise questions as to how often and to what magnitude continent to  
107 ocean transport occurs. This is important, particularly for Antarctica where the coastline  
108 stretches over 20,000 km in length and where prevailing strong winds through most of the year.  
109 Due to the sparsity of observations, the only way to estimate the mass of snow being blown off  
110 the coast of Antarctica is by using model parameterizations. Now, for the first time, satellite  
111 observations of blowing snow can help better ascertain the magnitude of this elusive quantity.  
112 Considering that the accuracy of model data is questionable over Antarctica, and the  
113 complicated factors that govern the onset of blowing snow, it is difficult to assess the accuracy  
114 of the parameterization of blowing snow sublimation and transport. Recently, methods have



115 been developed to detect the occurrence of blowing snow from direct satellite observations.  
116 Palm et al., (2011) show that blowing snow is widespread over much of Antarctica and, in all  
117 but the summer months, occurs over 50 % of the time over large areas of East Antarctica. In  
118 this paper, we present a technique that uses direct measurements of blowing snow from the  
119 CALIPSO satellite lidar combined with The Modern-Era Retrospective analysis for Research and  
120 Applications, Version 2 (MERRA-2) re-analysis fields of moisture, temperature and wind to  
121 quantify the magnitude of sublimation and mass transport occurring over most of Antarctica  
122 (north of 82° south). Section 2 discusses the method used to compute blowing snow sublimation  
123 from CALIPSO and MERRA-2 data. In Sect. 3 we show results and compare with previous  
124 estimates of sublimation. In Sect. 4 we examine sources of error and their approximate  
125 magnitudes. Summary and discussion follow in Sect. 5.

126

## 127 **2 Method**

128 The method developed for detection of blowing snow using satellite lidar data (both ICESat and  
129 CALIPSO) was presented in Palm et al., (2011). That work showed examples of blowing snow  
130 layers as seen by the calibrated, attenuated backscatter data measured by the CALIOP  
131 instrument on the CALIPSO satellite. CALIOP (Cloud-Aerosol Lidar with Orthogonal Polarization)  
132 is a two wavelength (532 and 1064 nm) backscatter lidar with depolarization at 532 nm and has  
133 been operating continuously since June of 2006 (Winker et. al., 2009). In the lower 5 km of the  
134 atmosphere, the vertical resolution of the CALIOP backscatter profile is 30 m. The CALIOP  
135 backscatter profiles are produced at 20 Hz, which is about a horizontal resolution of 330 m  
136 along track. The relatively strong backscattering produced by the earth's surface is used to  
137 identify the ground bin in each profile. After the ground signal is detected, each 20 Hz profile is  
138 examined for an elevated backscatter signal (above a pre-defined threshold) in the first bin  
139 above the ground. If found and the surface wind speed is greater than  $4 \text{ m s}^{-1}$ , successive bins  
140 above that are searched for a 80 % decrease in signal value, which is then the top of the layer.  
141 Limited by the vertical resolution of the signal, our approach has the ability to identify blowing  
142 snow layers that are roughly 15-20 m or more in thickness. Thus, drifting snow which is



143 confined to 10 m or less and occurs frequently over Antarctica would not be reliably detected.  
144 The signal from these layers is likely inseparable from the strong ground return. More  
145 information on the blowing snow detection algorithm can be found in Palm et al., (2011).  
  
146 For the work done in this paper we have created a new version of the blowing snow detection  
147 algorithm which strives to reduce the occurrence of false positive blowing snow detections. This  
148 is done by looking at both the layer average depolarization ratio and color ratio and limiting the  
149 top height of the layer to 500 m. If a layer is detected, but the top of the layer is above 500 m, it  
150 is not included as blowing snow. This height limit helped screen out diamond dust which often  
151 stretches for a few kilometers vertically and frequently reaches the ground. It was found that  
152 for most blowing snow layers, the depolarization and color ratio (1064/532) averaged about 0.4  
153 and 1.3, respectively (see Fig. 1). If the layer average color or depolarization ratios were out of  
154 pre-defined threshold limits, the layer was rejected. The layer average color ratio had to be  
155 greater than 1.0 and the depolarization ratio greater than 0.25. The large color ratio is  
156 consistent with model simulations for spherical ice particles (Bi et al., 2009). Further, logic was  
157 included to reduce misidentification of low cloud as blowing snow by limiting both the  
158 magnitude and height of the maximum backscatter signal in the layer. If the maximum signal  
159 were greater than  $2.0 \times 10^{-1} \text{ km}^{-1} \text{ sr}^{-1}$ , the layer was assumed cloud and not blowing snow. In  
160 addition, if the maximum backscatter, regardless of its value, occurs above 300 m, the layer is  
161 rejected. These changes to the blowing snow detection algorithm slightly decreased (few  
162 percent) the overall frequency of blowing snow detections, but we believe we have reduced the  
163 occurrence of false positives and the resulting retrievals are now more accurate.  
  
164 Typically, the blowing snow layers are 100–200 m thick, but can range from the minimum  
165 detectable height (20 - 30 m) to over 400 m in depth (Mahesh et al., 2003). Often they are seen  
166 to be associated with blowing snow storms that cover vast areas of Antarctica and can persist  
167 for days. Blowing snow can occur as frequently as 50 % of the time over large regions of East  
168 Antarctica in all months but December–February and as frequently as 75 % April through  
169 October (Palm et al., 2011). An example of a typical blowing snow layer as seen from the  
170 CALIOP backscatter data is shown in Fig. 1.



171 **2.1 Sublimation**

172 Sublimation of snow occurs at the surface but is greatly enhanced when the snow becomes  
173 airborne by the action of wind and turbulence. Once snow particles become airborne, their  
174 total surface area is exposed to the air. If the relative humidity of the ambient air is less than  
175 100 %, then sublimation will occur. The amount of sublimation is dictated by the number of  
176 snow particles in suspension and the relative humidity and temperature of the air. Thus, to  
177 estimate sublimation of blowing snow, we must be able to derive an estimate of the number  
178 density of blowing snow particles and have knowledge of atmospheric temperature and  
179 moisture within the blowing snow layer. The only source of the latter, continent wide at least, is  
180 from global or regional models or re-analysis fields. The number density of blowing snow  
181 particles can be estimated directly from the CALIOP calibrated, attenuated backscatter data if  
182 we can estimate the extinction within the blowing snow layer and have a rough idea of the  
183 blowing snow particle radius. The extinction can be estimated from the backscatter through an  
184 assumed extinction to backscatter ratio (lidar ratio) for the layer. The lidar ratio, though  
185 unknown, would theoretically be similar to that of cirrus clouds, which has been extensively  
186 studied. Work done by Josset et al., (2012) and Chen et al., (2002) shows that the extinction to  
187 backscatter ratio for cirrus clouds typically ranges between 25 and 30 with an average value of  
188 29. However, the ice particles that make up blowing snow are more rounded than the ice  
189 particles that comprise cirrus clouds and are on average somewhat smaller Walden et al.,  
190 (2003). For this paper, we use a value of 25 for the extinction to backscatter ratio.

191 Measurements of blowing snow particle size have been made by a number of investigators  
192 [Schmidt, 1982; Mann et al., 2000; Nishimura and Nemoto, 2005; Walden et al. 2003; Lawson et  
193 al., 2006; Gordon and Taylor, 2009], but they were generally made within the first few meters  
194 of the surface and may not be applicable to blowing snow layers as deep as those studied here.  
195 Most observations have shown a height dependence of particle size ranging from 100 to 200  
196  $\mu\text{m}$  in the lower tens of centimeters above the surface to 50–60  $\mu\text{m}$  near 10 m height  
197 (Nishimura and Nemoto, 2005). A notable exception is the result of Harder et al., (1996) at the  
198 South Pole, who measured the size of blowing snow particles during a blizzard by collecting



199 them on a microscope slide. They report nearly spherical particles with an average effective  
200 radius of 15  $\mu\text{m}$ , but the height at which the measurements were made is not reported. From  
201 surface observations made at the South Pole, Walden et al., (2003) and Lawson et al., (2006)  
202 report an average effective radius for blowing snow particles of 19 and 17  $\mu\text{m}$ , respectively.

203 While no field-measured values for particle radii above roughly 10 m height are available,  
204 modeling work indicates that they approach an asymptotic value of about 10-20  $\mu\text{m}$  at heights  
205 of 200 m or more (Dery and Yau, 1998). It is also reasonable to assume that snow particles that  
206 are high up in the layer are smaller since they have spent more time aloft and have had a  
207 greater time to sublimate. Based on the available data, we have defined particle radius ( $r(z)$ ,  
208  $\mu\text{m}$ ) as a linear function of height:

$$209 \quad r(z) = 40 - \frac{z}{20} \quad (1)$$

210 Thus, for the lowest level of CALIPSO retrieved backscatter (taken to be 15 m – the center of  
211 the first bin above the surface),  $r(15) = 39.25 \mu\text{m}$  and at the highest level (500 m),  $r(500) = 15$   
212  $\mu\text{m}$ .

213 The blowing snow particle number density  $N(z)$  (particles per cubic meter) is:

$$214 \quad N(z) = \frac{(\beta(z) - \beta_m(z)) S}{2\pi r^2(z)} \quad (2)$$

215 Where  $\beta(z)$  is the CALIPSO measured attenuated calibrated backscatter at height  $z$  (30 m  
216 resolution),  $\beta_m(z)$  is the molecular backscatter at height  $z$  and  $S$  is the extinction to backscatter  
217 ratio (25). Here  $\beta(z)$  represents the atmospheric backscatter profile through the blowing snow  
218 layer. Both  $\beta_m(z)$  and  $\beta(z)$  have units of  $\text{m}^{-1} \text{sr}^{-1}$ . We found that the values of  $N(z)$  obtained  
219 from Eq. (2) for the typical blowing snow layer range from about  $5.0 \times 10^4$  to  $1.0 \times 10^6$  particles  
220 per cubic meter. This is consistent with the blowing snow model results of Dery and Yau (2002)  
221 and the field observations of Mann et al., (2000). A plot of the average particle density for the  
222 blowing snow layer in Fig. 1 is shown in Fig. 2.



223 Once an estimate of blowing snow particle number density and radii are obtained, the  
 224 sublimation rate of the particles can be computed based on the theoretical knowledge of the  
 225 process. Following Dery and Yau, (2002), the blowing snow mixing ratio  $q_b$  (Kg ice / Kg air) is  
 226 given by:

$$227 \quad q_b(z) = \frac{4\pi \rho_{ice} r^3(z) N(z)}{3 \rho_{air}} \quad (3)$$

228 Or substituting for  $N(z)$  (Eq. 2):

$$229 \quad q_b(z) = \frac{2 \rho_{ice} r(z) [\beta(z) - \beta_m(z)] S}{3 \rho_{air}} \quad (4)$$

230 Where  $\rho_{ice}$  is the density of ice ( $917 \text{ kg m}^{-3}$ ), and  $\rho_{air}$  the density of air. Again following Dery and  
 231 Yau (2002) and others, the sublimation  $S_b$  at height  $z$  is computed from:

$$232 \quad S_b(z) = \frac{q_b(z) N_u [q_v(z)/q_{is}(z) - 1]}{2 \rho_{ice} r^2(z) [F_k(z) + F_d(z)]} \quad (5)$$

233 Or, letting  $\alpha(z)$  be the extinction and substituting for  $q_b(z)$ :

$$234 \quad S_b(z) = \frac{\alpha(z) N_u [q_v(z)/q_{is}(z) - 1]}{3 \rho_{ice} r(z) [F_k(z) + F_d(z)]} \quad (6)$$

235 Where Nu is the Nusslet number defined as:  $Nu = 1.79 + 0.606 Re^{0.5}$

236 with the Reynolds number being:  $Re = 2r(z) v_b / \nu$

237 where  $v_b$  is the snow particle fall speed (assumed here to be  $0.1 \text{ ms}^{-1}$ ) and  $\nu$  the kinematic  
 238 viscosity of air ( $1.512 \times 10^{-5} \text{ m}^2 \text{s}^{-1}$ ).  $q_v$  is the water vapor mixing ratio of the air (obtained from  
 239 model data),  $q_{is}$  is the saturation mixing ratio with respect to ice, and  $F_k$  and  $F_d$  are the heat  
 240 conduction and diffusion terms ( $\text{m s Kg}^{-1}$ ):

$$241 \quad F_k = \left( \frac{L_s}{R_v T} - 1 \right) \frac{L_s}{K T}$$

$$F_d = \frac{R_v T}{D e_i(T)}$$



242 Where  $L_s$  is the latent heat of sublimation ( $2.839 \times 10^6$  J/Kg),  $R_v$  is the individual gas constant for  
243 water vapor ( $461.5 \text{ J Kg}^{-1} \text{ K}^{-1}$ ),  $T$  is temperature (K),  $K$  is the thermal conductivity of air, and  $D$   
244 the coefficient of diffusion of water vapor in air (both  $D$  and  $K$  are functions of temperature (see  
245 Rogers and Yau, 1989)).  $S_b$  has units of  $\text{Kg Kg}^{-1} \text{ s}^{-1}$ . This can be interpreted as the mass of snow  
246 sublimated per mass of air per second.

247 Then the column integrated blowing snow sublimation is:

$$248 Q_s = \rho_{air} \int_{z=0}^{Z_{top}} S_b(z) dz \quad (7)$$

249 Where  $Z_{top}$  is the top of the blowing snow layer and  $dz$  is 30 meters.  $Q_s$  has units of  $\text{Kg m}^{-2} \text{ s}^{-1}$ .  
250 Conversion to mm snow water equivalent (swe) per day is performed by multiplying by a  
251 conversion factor:

$$252 \rho' = 10^3 N_s / \rho_{ice} \quad (8)$$

253 Where  $N_s$  is the number of seconds in a day (86,400). The total sublimation amount in mm swe  
254 per day is then:

$$255 Q' = \rho' Q_s \quad (9)$$

256 This computation is performed for every blowing snow detection along the CALIPSO track over  
257 Antarctica. A  $1 \times 1$  degree grid is then established over the Antarctic continent and each  
258 sublimation calculation ( $Q'$ ) is added to its corresponding grid box over the length of time being  
259 considered (i.e. a year or month). This value is then normalized by the total number of CALIPSO  
260 observations that occurred for that grid box over the time span. The total number of  
261 observations includes all CALIPSO shots within the grid box for which a ground return was  
262 detected, regardless of whether blowing snow was detected for that shot or not. Thus, the  
263 normalization factor is the total number of shots with ground return detected for that box and  
264 is always greater than the number of blowing snow detections (which equals the number of  
265 sublimation retrievals). In order for the blowing snow detection algorithm to function, it must  
266 first detect the position of the ground return in the backscatter profile. If it cannot do so, it is



267 not considered an observation. Over the interior of Antarctica, failure to detect the surface  
268 does not occur often as cloudiness is less than 10 % and most clouds are optically thin. Near the  
269 coasts, optically thick clouds become more prevalent. This approach will result in higher  
270 sublimation values for those grid boxes that contain a lot of blowing snow detections and vice  
271 versa (as opposed to just taking the average of the sublimation values for a grid box).

272

## 273 **2.2 Transport**

274 The transport of blowing snow is computed using the CALIPSO retrievals of blowing snow  
275 mixing ratio and the MERRA-2 winds. A transport value is computed at each 30 m bin level and  
276 integrated through the depth of the blowing snow layer:

$$277 Q_t = \rho_{air} \int_{z=0}^{Z_{top}} q_b(z) u(z) dz \quad (10)$$

278 Where  $q_b(z)$  is the blowing snow mixing ratio from Eq. (3) and  $u(z)$  is the MERRA-2 wind speed  
279 at height  $z$  and  $Q_t$  has units of  $\text{kg m}^{-1} \text{ s}^{-1}$ . The wind speed is linearly interpolated from the  
280 nearest two model levels. As with the sublimation, these values are gridded and normalized by  
281 the total number of observations. The transport values are computed for each month of the  
282 year by summing daily values and then multiplying by the number of seconds in the month  
283 (resulting units of  $\text{kg m}^{-1}$ ). The monthly values are then summed to obtain a yearly amount. A  
284 further conversion is performed to produce units of  $\text{Gt m}^{-1} \text{ yr}^{-1}$  by dividing by  $10^{12}$  (1000 kg per  
285 metric ton and  $10^9$  tons per Gt).

## 286 **3 Results**

### 287 **3.1 Sublimation**

288 Figure 3 shows the average blowing snow frequency and corresponding total annual blowing  
289 snow sublimation over Antarctica for the period 2007–2015. The highest values of sublimation  
290 are along and slightly inland of the coast. Notice that this is not necessarily where the highest



291 blowing snow frequencies are located. Sublimation is highly dependent on the air temperature  
292 and relative humidity. For a given value of the blowing snow mixing ratio ( $q_b$ ), the warmer and  
293 drier the air, the greater the sublimation. In Antarctica, it is considerably warmer along the  
294 coast but one would not necessarily conclude that it is drier there. However, other authors  
295 have noted that the katabatic winds, flowing essentially downslope, will warm and dry the air  
296 as they descend (Gallee, 1998, and others). We have examined the MERRA-2 relative humidity  
297 (with respect to ice) and indeed, according to the model, it is usually drier along the coast. The  
298 model data often shows 90 to 100 % (or even higher) relative humidity for interior portions of  
299 Antarctica, while along the coast it is often 60 % or less. It should be noted, however, that this  
300 model prediction has never been validated through observations. The combination of warmer  
301 and drier air makes a big difference in the sublimation as shown in Fig. 4. For a given relative  
302 humidity the sublimation can increase by almost a factor of 100 as temperature increases from  
303 -50 to -10 °C. For temperatures greater than -20 °C, sublimation is very dependent on relative  
304 humidity, but this dependence lessens somewhat at colder temperatures. Continental interior  
305 areas with very high blowing snow frequency that approach 75 % (like the Mega Dune region in  
306 East Antarctica) exhibit fairly low values of sublimation because it is very cold and the model  
307 relative humidity is high.

308 Figure 5 shows the annual total sublimation for years 2007–2015. It is evident that the  
309 sublimation pattern or magnitude does not change much from year to year. The overall spatial  
310 pattern of sublimation is similar to the model prediction of Dery and Yau, (2002) with our  
311 results showing noticeably greater amounts in the Antarctic interior and generally larger values  
312 near the coast. As previously noted, most sublimation occurs near the coast due mainly to the  
313 warmer temperatures. The areas of sublimation maximums near the coast are consistently in  
314 the same location year to year, indicating that these areas may experience more blowing snow  
315 episodes and possibly more precipitation (availability of snow to become airborne). It is  
316 interesting to compare the sublimation pattern with current estimates of Antarctic  
317 precipitation. Precipitation is notoriously difficult to quantify over Antarctica due to the scarcity  
318 of observations and strong winds producing drifting and blowing snow which can be  
319 misidentified as precipitation. Precipitation is often measured by looking at ice cores or is



320 estimated by models. But perhaps the most complete (non-model) measure of Antarctic  
321 precipitation come from the CloudSat mission. Palerme et al., (2014) used CloudSat data to  
322 construct a map of Antarctic precipitation over the entire continent (north of 82 S). They  
323 showed that along the East Antarctic coast and slightly inland, precipitation ranges from 500 to  
324 700 mm swe  $\text{yr}^{-1}$  and decreases rapidly inland to less than 50 mm  $\text{yr}^{-1}$  in most areas south of 75  
325 S. Their precipitation pattern is in general agreement with the spatial pattern of our  
326 sublimation results and the magnitude of our sublimation estimates is in general less than the  
327 precipitation amount, with a few exceptions. These occur mostly inland in regions of high  
328 blowing snow frequency such as the Megadune region and in the general area of the Lambert  
329 glacier. In these regions, our sublimation estimates exceed the CloudSat yearly precipitation  
330 estimates. When this occurs, it is likely that either the precipitation estimate is low or the  
331 sublimation estimate is too high. Otherwise it would indicate a net negative mass balance for  
332 the area unless transport of snow into the region accounted for the difference.

333 Table 1 shows the average sublimation over all grid cells in snow water equivalent and the  
334 integrated sublimation amount over the Antarctic continent (north of 82S) for the CALIPSO  
335 period in  $\text{Gt yr}^{-1}$ . Note that the 2006 data include only months June–December (CALIOP began  
336 operating in June, 2006) and the 2016 data are only up through October, and do not include the  
337 month of February (CALIOP was not operating). To obtain the integrated amount, we take the  
338 year average swe (column 1) multiplied by the surface area of Antarctica north of 82S and the  
339 density of ice. The average integrated value for the 9 year period 2007–2015 of  $419 \text{ Gt yr}^{-1}$  is  
340 significantly greater than (about twice) values in the literature obtained from model  
341 parameterizations (Lenaerts 2012b). Note also that these figures do not include the area  
342 poleward of 82S, the southern limit of CALIPSO observations. If included, and the average  
343 sublimation rate over this area were just 4 mm swe per year, this would increase the  
344 sublimation total by  $10 \text{ Gt yr}^{-1}$ . Gallee (1998) used a model to compute blowing snow  
345 sublimation over Antarctica and obtained a continent-wide average value of 0.087 mm per day.  
346 Further he postulated that If this were constant over a year, it would amount to about 32 mm  
347 swe and if all of it were deposited in the ocean it would account for  $1.3 \text{ mm yr}^{-1}$  of sea level rise.  
348 The same logic applied to our results would yield a  $1.7 \text{ mm yr}^{-1}$  seal level rise.



349 Our results (Table 1) show somewhat of a decreasing trend to the data with the years 2007 and  
350 2008 having the highest sublimation values while 2014 and 2015 have the lowest. If this trend is  
351 real, it is not clear what is causing it. The frequency of blowing snow is relatively constant over  
352 this period when integrated over the continent (not shown). Other factors that could cause a  
353 decrease in sublimation are colder temperatures, increased humidity, or decreased blowing  
354 snow particle concentration (which would equate to a decreased average layer integrated  
355 backscatter).

356 Palerme et al., (2014) has shown that the mean snowfall rate over Antarctica (north of 82 S)  
357 from August 2006 to April 2011 is  $171 \text{ mm yr}^{-1}$ . The average yearly snow water equivalent  
358 sublimation from Table I is the average sublimation over the continent (also north of 82 S). For  
359 the same time period, our computed CALIPSO-based average blowing snow sublimation is  
360 about  $50 \text{ mm yr}^{-1}$ . This means that on average, over one third of the snow that falls over  
361 Antarctica is lost to sublimation through the blowing snow process. In comparison surface  
362 sublimation (sublimation of snow on the surface) is considered to be relatively small (about a  
363 tenth of airborne sublimation) except in summer (Lenearts 2012a, 2012b).

### 364 **3.2 Transport**

365 Transport of snow via the wind is generally important locally and does not constitute a large  
366 part of the ice sheet mass balance in Antarctica. There are areas where the wind scours away all  
367 snow that falls producing a net negative mass balance (i.e. blue ice areas), but in general, the  
368 snow is simply moved from place to place over most of the continent. At the coastline,  
369 however, this is not the case. There, persistent southerly winds can carry airborne snow off the  
370 continent. This can be seen very plainly in Fig. 6 which is a MODIS false color (RGB = 2.1, 2.1, .85  
371  $\mu\text{m}$ ) image of a large area of blowing snow covering an area about the size of Texas in East  
372 Antarctica. We have found this false color technique to be the best way to visualize blowing  
373 snow from passive sensors. The one drawback is that sunlight is required. In the figure, blowing  
374 snow shows up as a dirty white, the ice/snow surface (in clear areas) is blue and clouds are  
375 generally a brighter white. Also shown in Fig. 6 are two CALIPSO tracks (yellow lines) and their



376 associated retrieved blowing snow backscatter (upper and lower images of CALIOP  
377 backscatter). Note that the yellow track lines are drawn only where blowing snow was detected  
378 by CALIOP and that not all the CALIOP blowing snow detections are shown. The green dots  
379 denote the coastline. Plainly seen along the coast near longitude 145–150E is blowing snow  
380 being carried off the continent. In this case, topography might have played a role to funnel the  
381 wind in those specific areas. Figure 7 shows a zoomed in image of this area with the red lines  
382 indicating the approximate position of the coastline. Also note that, as evidenced by the times  
383 of the MODIS images, this transport began on or before October 13 at 23:00 UTC and continued  
384 for at least 7 hours. This region is very close to the area of maximum sublimation seen in Fig. 3  
385 and shown to be quite stable from year to year in Fig. 5. Undoubtedly, this continent to ocean  
386 transport also occurs in other coastal areas of Antarctica and most often during the dark winter  
387 (when MODIS could not see it).

388 In an attempt to better understand the magnitude of this phenomena, we have computed the  
389 amount of snow mass being blown off the continent by computing the transport at 342 points  
390 evenly spaced (about 70 km apart) along the Antarctic coast using only the v component of the  
391 wind. If the v component is positive, then the wind is from south to north. The transport (Eq.  
392 (10) using only the v wind component) is computed at each coastal location and then summed  
393 over time at that location. The resulting transport is then summed over each coastal location to  
394 arrive at a continent-wide value of transport from continent to ocean. Of course this assumes  
395 that the coastline is oriented east-west everywhere. This is true of a large portion of Antarctica  
396 but there are regional exceptions. Thus we view the results shown in Table II to be an upper  
397 limit of the actual continent to ocean transport. Evident from Table 2 is that most of the  
398 transport for East Antarctica occurs in a relatively narrow corridor, with on average over half  
399 (51 %) of the transport occurring between 135E and 160E. This is obviously due to the very  
400 strong and persistent southerly winds (see Fig. 10) and high blowing snow frequency in this  
401 region and is consistent with the conclusions of Scarchilli et al., (2010). In West Antarctica, an  
402 even greater fraction (60 %) of the transport off the coast occurs between 80W and 120W.



403 In Fig. 8 we show the magnitude of blowing snow transport for the 2007–2015 timeframe in Mt  
404  $\text{km}^{-1} \text{ yr}^{-1}$  as computed from Eq. (10). The magnitude of snow transport, as expected, closely  
405 resembles the overall blowing snow frequency pattern as shown in Fig. 3. The maximum values  
406 (white areas in Fig. 8) exceed about  $3 \times 10^6$  tons of snow per km per year. In Figs. 9 and 10 we  
407 display the MERRA-2 average 10 m wind speed and direction for the years 2007–2015. By  
408 inspection of Figs. 8 and 10 it is seen that the overall transport in East Antarctica is generally  
409 from south to north and obviously dominated by the katabatic wind regime. It is immediately  
410 apparent that the average wind speed and direction does not change much from year to year,  
411 with the former helping to explain why the average continent-wide blowing snow frequency is  
412 also nearly constant from year to year (not shown).

413 **4. Error Analysis**

414 There are a number of factors that can affect the accuracy of the results presented in this work.  
415 These include:

416 1) Error in the calibrated backscatter and conversion to extinction  
417 2) Errors in the assumed size of blowing snow particles  
418 3) Not correcting for possible attenuation above the blowing snow layer  
419 4) Misidentification of some layers as blowing snow when in fact they were not (false positives)  
420 5) Failure to detect some layers (false negatives)  
421 6) Errors in the MERRA-2 temperature and moisture data  
422 7) Limited spatial sampling

423 The magnitude of some of these can be estimated, others are hard to quantify. For instance, 1),  
424 2) and 6) are directly involved in the calculation of sublimation (Eq. 6). The error in extinction,  
425 particle radius, temperature and moisture can be estimated. The error associated with 3) is  
426 probably very small over the interior of Antarctica, but could be appreciable nearer the  
427 coastline. In the interior, clouds are a rare occurrence and when present are usually optically  
428 thin. Cloudiness increases dramatically near the coast both in terms of frequency and optical  
429 depth. Here the effect of overlying attenuating layers could be appreciable in that it would



430 reduce the backscatter of the blowing snow layer and the derived extinction. This in turn would  
431 lead to a lower blowing snow mixing ratio and thus lower sublimation and transport.

432 There is a further point to be made with respect to clouds that relates to 5) above. The method  
433 we use to detect blowing snow will not work in the presence of overlying, fully attenuating  
434 clouds. It is reasonable to suspect that cyclonic storms which impinge upon the Antarctic coast  
435 and travel some distance inland would be associated with optically thick clouds and contain  
436 both precipitating and blowing snow. Our method would not be able to detect blowing snow  
437 during these storms, but we would not count such cases as "observations", since the ground  
438 would not be detected. The point is, blowing snow probably occurs often in wintertime  
439 cyclones, but we are not able to detect it. This could lead to an under prediction of blowing  
440 snow occurrence, especially near the coast. Also, blowing snow layers less than 20 - 30 m thick  
441 would also likely be missed. It is not clear how often these layers occur, but they are known to  
442 exist and missing them will produce an underestimate of blowing snow sublimation and  
443 transport amounts. With regard to spatial sampling (7 above), unlike most passive sensors,  
444 CALIPSO obtains only point measurements along the spacecraft track at or near nadir. On a  
445 given day, sampling is poor. CALIPSO can potentially miss a large portion of blowing snow  
446 storms such as is evidenced from inspection of Fig. 6. We have seen many examples of such  
447 storms in both the MODIS and CALIPSO record. Quantifying the effect of poor sampling on  
448 sublimation estimates would be difficult but should be pursued in future work.

449 In an effort to quantify the error in our sublimation estimates, here we assume the extinction  
450 error to be 20 %, the particle radius error 10 % and the temperature and moisture error 5 %  
451 each. In Eq. (6) these terms are multiplicative. The total error in sublimation is then:

$$452 \pm 1 - (0.8 * 0.9 * 0.95 * 0.95) = \pm 0.35$$

453 This indicates that the sublimation values derived in this work should be considered to have an  
454 error bar of  $\pm 35$  %. The error in computed transport involves error in wind speed and the  
455 blowing snow mixing ratio, the latter being dependent on extinction and particle size. If we



456 assume wind speed has an error of 20 %, extinction 20 % and particle size 10 %, the total error  
457 in transport is:

458  $\pm 1 - (0.8 * 0.8 * 0.9) = \pm 0.42$

459 **5. Summary and Discussion**

460 This paper presents the first estimates of blowing snow sublimation and transport over  
461 Antarctica that are based on actual observations of blowing snow layers from the CALIOP space  
462 borne lidar. We have used the CALIOP blowing snow retrievals combined with MERRA-2 model  
463 re-analyses of temperature and moisture to compute the temporal and spatial distribution of  
464 blowing snow sublimation and transport over Antarctica for the first time. The results show that  
465 the maximum sublimation, with annual values exceeding 250 mm swe, occurs within roughly  
466 200 km of the coast even though the maximum frequency of blowing snow most often occurs  
467 considerably further inland. This is a result of the warmer and drier air near the coast (at least  
468 in the MERRA-2 re-analysis data) which substantially increases the sublimation. In the interior,  
469 extremely cold temperatures and high model relative humidity lead to greatly reduced  
470 sublimation. However, the values obtained in parts of the interior (notably the Megadune  
471 region of East Antarctica - roughly 75 to 82S and 120 to 160E) are considerably higher than  
472 prior model estimates of Dery and Yau (2002) or Lenaerts et al., 2012a). This is most likely due  
473 to the very high frequency of occurrence of blowing snow as detected from CALIOP data in this  
474 region which is not necessarily captured in models (Lenaerts et al., 2012b).

475 The overall spatial pattern of blowing snow sublimation is consistent with previous modelling  
476 studies (Dery and Yau, 2002 and Lenaerts et al., 2012a). However, we find the Antarctic  
477 continent-wide integrated blowing snow sublimation to be about twice the amount of previous  
478 studies such as Lenaerts et al., (2012a) ( $393 \pm 138$  vs roughly  $190 \text{ Gt yr}^{-1}$ ), even though the  
479 observations include only the area north of 82° S. The maximum in sublimation is about 250  
480 mm swe per year near the coast between longitudes 140E and 150E and seems to occur  
481 regularly throughout the 11 year data record. One reason for the higher sublimation values in  
482 this study is that the average blowing snow layer depth as determined from the CALIOP



483 measurements is 120 m. Layers as high as 200 - 300 m are not uncommon. It is likely that  
484 models such as those cited above do not always capture the full depth of blowing snow layers,  
485 thus producing a smaller column-integrated sublimation amount. Another reason for  
486 differences between our result and previous model estimates lies in the fact that we only  
487 compute sublimation from blowing snow layers that are known to exist (meaning they have  
488 been detected from actual backscatter measurements). Models, on the other hand, must infer  
489 the presence of blowing snow from pertinent variables within the model. The existence of  
490 blowing snow is not easy to predict. It is a complicated function of the properties of the  
491 snowpack, surface temperature, relative humidity and wind speed. Snowpack properties  
492 include the dendricity, sphericity, grain size and cohesion, all of which can change with the age  
493 of the snow. In short, it is very difficult for models to predict exactly when and where blowing  
494 snow will occur, much less the depth that blowing snow layer will attain.

495 The spatial pattern of the transport of blowing snow follows closely the pattern of blowing  
496 snow frequency. The maximum transport values are about 5 Megatons per km per year and  
497 occur in the Megadune region of East Antarctica with other locally high values at various  
498 regions near the coast that generally correspond to the maximums in sublimation. We  
499 attempted to quantify the amount of snow being blown off the Antarctic continent by  
500 computing the transport along the coast using only the  $v$  component of the wind. While this  
501 may produce an overestimate of the transport (since the Antarctic coast is not oriented east-  
502 west everywhere), we find the amount of snow blown off the continent to be significant and  
503 fairly constant from year to year. The average off-continent transport for the 9 year period  
504 2007–2015 was  $3.68 \text{ Gt yr}^{-1}$  with about two thirds of that coming from East Antarctica and over  
505 one third from a relatively small area between longitudes 135E and 160E.

506 Over the nearly 11 years of data, the inter-annual variability of continent wide sublimation  
507 (Table 1) can be fairly large – 10 to 15 % - and likely the result of precipitation variability. There  
508 seems to be a weak trend to the sublimation data with earlier years having greater sublimation  
509 than more recent years. However, based on the likely magnitude of error in the sublimation  
510 estimates, the trend cannot be considered statistically significant.



511 **Data Availability**

512 The CALIPSO calibrated attenuated backscatter data used in this study can be obtained from  
513 the NASA Langley Atmospheric Data Center at: [https://earthdata.nasa.gov/about/daacs/daac-](https://earthdata.nasa.gov/about/daacs/daac-asdc)  
514 [asdc](https://earthdata.nasa.gov/about/daacs/daac-asdc). CALIPSO Science Team (2015), CALIPSO/CALIOP Level 1B, Lidar Profile Data,  
515 version 3.30, Hampton, VA, USA: NASA Atmospheric Science Data Center (ASDC), Accessed  
516 at various times during 2016 at doi: 10.5067/CALIOP/CALIPSO/CAL\_LID\_L1-ValStage1-V3-  
517 30\_L1B-003.30

518

519 The MERRA-2 data are available from the Goddard Earth Sciences Data and Information  
520 Services Center (GESDISC) at: [https://disc.gsfc.nasa.gov/datasets/merra\\_2\\_data\\_release](https://disc.gsfc.nasa.gov/datasets/merra_2_data_release).

521 The blowing snow data (layer backscatter, height, etc.) are available through the corresponding  
522 author and will be made publicly available through the NASA Langley Atmospheric Data Center  
523 in the near future.

524 **Acknowledgements**

525 This research was performed under NASA contracts NNH14CK40C and NNH14CK39C. The  
526 authors would like to thank Dr Thomas Wagner and Dr David Considine for their support and  
527 encouragement. The CALIPSO data used in this study were the DOI:  
528 10.5067/CALIOP/CALIPSO/LID\_L1-ValStage1-V3-40\_L1B-003.40 data product obtained from the  
529 NASA Langley Research Center Atmospheric Science Data Center. We also acknowledge the  
530 Global Modeling and Assimilation Office (GMAO) at Goddard Space Flight Center who supplied  
531 the MERRA-2 data and the AMPS data were kindly supplied by Julien Nicolas of the Byrd Polar  
532 and Climate Research Center at Ohio State University.

533 **References**

534 Bi, L., Yang, P., Kattawar, G. W., Baum, B. A., Hu, Y. X., Winker, D. M., Brock, R. S., and J. Q. Lu, J.  
535 Q.: Simulation of the color ratio associated with the backscattering of radiation by ice particles



536 at the wavelengths of 0.532 and 1.064  $\mu\text{m}$ , *J. Geophys. Res.*, 114, D00H08,  
537 doi:10.1029/2009JD011759, 2009.

538 Bintanja, R., and Krikken, F.: Magnitude and pattern of Arctic warming governed by the  
539 seasonality of radiative forcing, *Sci. Rep.-Uk*, 6, doi: 10.1038/srep38287, 2016.

540 Bowling, L. C., Pomeroy, J. W., and Lettenmaier, D. P.: Parameterization of blowing-snow  
541 sublimation in a macroscale hydrology model, *J Hydrometeor.*, 5, 745-762, doi: 10.1175/1525-  
542 7541(2004)005<0745:Pobsia>2.0.Co;2, 2004.

543 Bromwich, D. H., Nicolas, J. P., Monaghan, A. J., Lazzara, M. A., Keller, L. M., Weidner, G. A., and  
544 Wilson, A. B.: Central West Antarctica among the most rapidly warming regions on Earth, *Nat.*  
545 *Geosci.*, 6, 139-145, doi: 10.1038/Ngeo1671, 2013.

546 Bromwich, D. H.: Snowfall in high southern latitudes. *Rev Geophys* 26:149–168, 1988

547 Chen, W. N., Chiang, C. W., and Nee, J. B.: Lidar ratio and depolarization ratio for cirrus clouds,  
548 *Appl. Optics*, 41, 6470-6476, doi: 10.1364/Ao.41.006470, 2002.

549 Church, J. A., Clark, P. U., Cazenave, A., Gregory, J. M., Jevrejeva, S., Levermann, A., Merrifield,  
550 M. A., Milne, G. A., Nerem, R. S., Nunn, P. D., Payne, A. J., Pfeffer, W. T., Stammer, D., and  
551 Unnikrishnan, A. S.: Sea level change, in: *Climate change 2013: The Physical science basis*.  
552 Contribution of working group I to fifth assessment report of the Intergovernmental panel of  
553 climate change, edited by: Stocker, T. F., Qin, D., Plattner, G. K., Tignor, M., Allen, S. K.,  
554 Boschung, J., Nauels, A., Xia, Y., Bex, V., and Midgley, P. M., Cambridge University Press,  
555 Cambridge, UK and New York, USA, 2013.

556 Das, I., Bell, R. E., Scambos, T. A., Wolovick, M., Creyts, T. T., Studinger, M., Frearson, N.,  
557 Nicolas, J. P., Lenaerts, J. T. M., and van den Broeke, M. R.: Influence of persistent wind scour  
558 on the surface mass balance of Antarctica, *Nat. Geosci.*, 6, 367-371, doi: 10.1038/Ngeo1766,  
559 2013.



560 Dery, S. J., and Yau, M. K.: Large-scale mass balance effects of blowing snow and surface  
561 sublimation, *J. Geophys. Res.-Atmos.*, 107, doi: 10.1029/2001jd001251, 2002.

562 Dery, S. J. and Yau, M. K.: Simulation of Blowing Snow in the Canadian Arctic Using a Double-  
563 Moment Model, *Boundary-Layer Meteorology*, 99, 297–316, 2001.

564 Dery, S. J. and M.K. Yau, M. K.: A Bulk Blowing Snowmodel, *Boundary-Layer Meteorology*, 93,  
565 237–251, 1999.

566 Dery, S. J., Taylor, P. A., Xiao, J.: The Thermodynamic Effects of Sublimating, Blowing Snow in  
567 the Atmospheric Boundary Layer, Dept. of Atmospheric and Oceanic Sciences, McGill  
568 University, 805 Sherbrooke St. W., Montréal, Québec, H3A 2K6 Canada, *Boundary-Layer  
569 Meteorology*, 89, 251–283, 1998.

570 Frezzotti, M., Gandolfi, S., and Urbini, S.: Snow megadunes in Antarctica: Sedimentary structure  
571 and genesis, *J. Geophys. Res.-Atmos.*, 107, doi: 10.1029/2001jd000673, 2002.

572 Gallée, H.: A simulation of blowing snow over the Antarctic ice sheet, *Ann Glaciol.*, 26, 203–205,  
573 1998.

574 Gordon, M., and Taylor, P. A.: Measurements of blowing snow, Part I: Particle shape, size  
575 distribution, velocity, and number flux at Churchill, Manitoba, Canada, *Cold Reg. Sci. Technol.*,  
576 55, 63–74, doi: 10.1016/j.coldregions.2008.05.001, 2009.

577 Harder, S. L., Warren, S. G., Charlson, R. J., and Covert, D. S.: Filtering of air through snow as a  
578 mechanism for aerosol deposition to the Antarctic ice sheet, *J. Geophys. Res.-Atmos.*, 101,  
579 18729–18743, doi: 10.1029/96jd01174, 1996.

580 Josset, D., Pelon, J., Garnier, A., Hu, Y. X., Vaughan, M., Zhai, P. W., Kuehn, R., and Lucker, P.:  
581 Cirrus optical depth and lidar ratio retrieval from combined CALIPSO-CloudSat observations  
582 using ocean surface echo, *J. Geophys. Res.-Atmos.*, 117, doi: 10.1029/2011jd016959, 2012.



583 King, J. C., Anderson, P. S., and Mann, G. W.: The seasonal cycle of sublimation at Halley,  
584 Antarctica, *J. Glaciol.*, 47, 1-8, doi: 10.3189/172756501781832548, 2001.

585 Lawson, R. P., Baker, B. A., Zmarzly, P., O'Connor, D., Mo, Q. X., Gayet, J. F., and Shcherbakov,  
586 V.: Microphysical and optical properties of atmospheric ice crystals at South Pole station, *J.*  
587 *Appl. Meteor. Climatol.*, 45, 1505-1524, doi: 10.1175/Jam2421.1, 2006.

588 Lenaerts, J. T. M., van den Broeke, M. R., Dery, S. J., van Meijgaard, E., van de Berg, W. J., Palm,  
589 S. P., and Rodrigo, J. S.: Modeling drifting snow in Antarctica with a regional climate model: 1.  
590 Methods and model evaluation, *J. Geophys. Res.-Atmos.*, 117, doi: 10.1029/2011jd016145,  
591 2012a.

592 Lenaerts, J. T. M., van den Broeke, M. R., van de Berg, W. J., van Meijgaard, E., and Munneke, P.  
593 K.: A new, high-resolution surface mass balance map of Antarctica (1979-2010) based on  
594 regional atmospheric climate modeling, *Geophys. Res. Lett.*, 39, doi: 10.1029/2011gl050713,  
595 2012b.

596 Mahesh, A., Eager, R., Campbell, J. R., and Spinhirne, J. D.: Observations of blowing snow at the  
597 South Pole, *J. Geophys. Res.*, 108(D22), 4707, doi:10.1029/2002JD003327, 2003.

598 Mann, G. W., Anderson, P. S., and Mobbs, S. D.: Profile measurements of blowing snow at  
599 Halley, Antarctica, *J. Geophys. Res.-Atmos.*, 105, 24491-24508, doi: 10.1029/2000jd900247,  
600 2000.

601 Nishimura, K., and Nemoto, M.: Blowing snow at Mizuho station, Antarctica, *Philos. T Roy Soc.*  
602 A, 363, 1647-1662, doi: 10.1098/rsta.2005.1599, 2005.

603 Palerme, C., Kay, J. E., Genthon, C., L'Ecuyer, T., Wood, N. B., and Claud, C.: How much snow  
604 falls on the Antarctic ice sheet?, *Cryosphere*, 8, 1577-1587, doi: 10.5194/tc-8-1577-2014, 2014.



605 Palm, S. P., Yang, Y. K., Spinhirne, J. D., and Marshak, A.: Satellite remote sensing of blowing  
606 snow properties over Antarctica, *J. Geophys. Res.-Atmos.*, 116, doi: 10.1029/2011jd015828,  
607 2011.

608 Pomeroy, J. W., Gray, D. M., and Landine, P. G.: The Prairie Blowing Snow Model -  
609 Characteristics, Validation, Operation, *J. Hydrol.*, 144, 165-192, doi: 10.1016/0022-  
610 1694(93)90171-5, 1993.

611 Pomeroy, J. W., Marsh, P., and Gray, D. M.: Application of a distributed blowing snow model to  
612 the arctic, *Hydrol. Process.*, 11, 1451-1464, 1997.

613 Przybylak, R.: Recent air-temperature changes in the Arctic, *Annals of Glaciology*, Vol 46, 2007,  
614 46, 316-324, doi: 10.3189/172756407782871666, 2007.

615 Rogers, R. R., and Yau, M. K.: A Short Course in Cloud Physics, 3<sup>rd</sup>. ed., Pergamon Press, 290 pp.,  
616 1989.

617 Scarchilli, C., Frezzotti, M., Grigioni, P., De Silvestri, L., Agnoletto, L., and Dolci, S.: Extraordinary  
618 blowing snow transport events in East Antarctica, *Clim. Dynam.*, 34, 1195-1206, doi:  
619 10.1007/s00382-009-0601-0, 2010.

620 Schmidt, R. A.: Vertical profiles of wind speed, snow concentration and humidity and blowing  
621 snow, *Boundary-layer Meteorol.*, 23, 223-246, 1982.

622 Steig, E. J., Schneider, D. P., Rutherford, S. D., Mann, M. E., Comiso, J. C., and Shindell, D. T.:  
623 Warming of the Antarctic ice-sheet surface since the 1957 International Geophysical Year,  
624 *Nature*, 457, 459-462, doi: 10.1038/nature07669, 2009.

625 Tabler, R. D., Benson, C. S., Santana, B. W., and Ganguly, P.: Estimating Snow Transport from  
626 Wind-Speed Records - Estimates Versus Measurements at Prudhoe Bay, Alaska, *Proceedings of*  
627 *the Western Snow Conference : Fifty-Eighth Annual Meeting*, 61-72, 1990.



628 Tabler, R. D.: Estimating the transport and evaporation of blowing snow Snow Management on  
629 the Great Plains, July 1985, Swift Current, Sask, Great Plains Agricultural Council Publication No.  
630 73, University of Nebraska, Lincoln, NE, 1975, pp. 85-105.

631 Van den Broeke, M., Konig-Langlo, G., Picard, G., Munneke, P. K., and Lenaerts, J.: Surface  
632 energy balance, melt and sublimation at Neumayer Station, East Antarctica, *Antarct. Sci.*, 22,  
633 87-96, doi: 10.1017/S0954102009990538, 2010.

634 Walden, V. P., Warren, S. G., and Tuttle, E.: Atmospheric ice crystals over the Antarctic Plateau  
635 in winter, *J. Appl. Meteor. Climatol.*, 42, 1391-1405, doi: 10.1175/1520-  
636 0450(2003)042<1391:Aicota>2.0.Co;2, 2003.

637 Winker, D. M., Vaughan, M. A., Omar, A., Hu, Y. X., Powell, K. A., Liu, Z. Y., Hunt, W. H., and  
638 Young, S. A.: Overview of the CALIPSO mission and CALIOP data processing algorithms, *J. Atmos.*  
639 *Oceanic Technol.*, 26, 2310-2323, doi: 10.1175/2009jtecha1281.1, 2009.



640 Table I. The year average sublimation per year (average off all grid boxes) and the integrated  
 641 sublimation over the Antarctic continent (north of 82S). \*2006 and 2016 consist of only 7 and 9  
 642 months of observations, respectively.

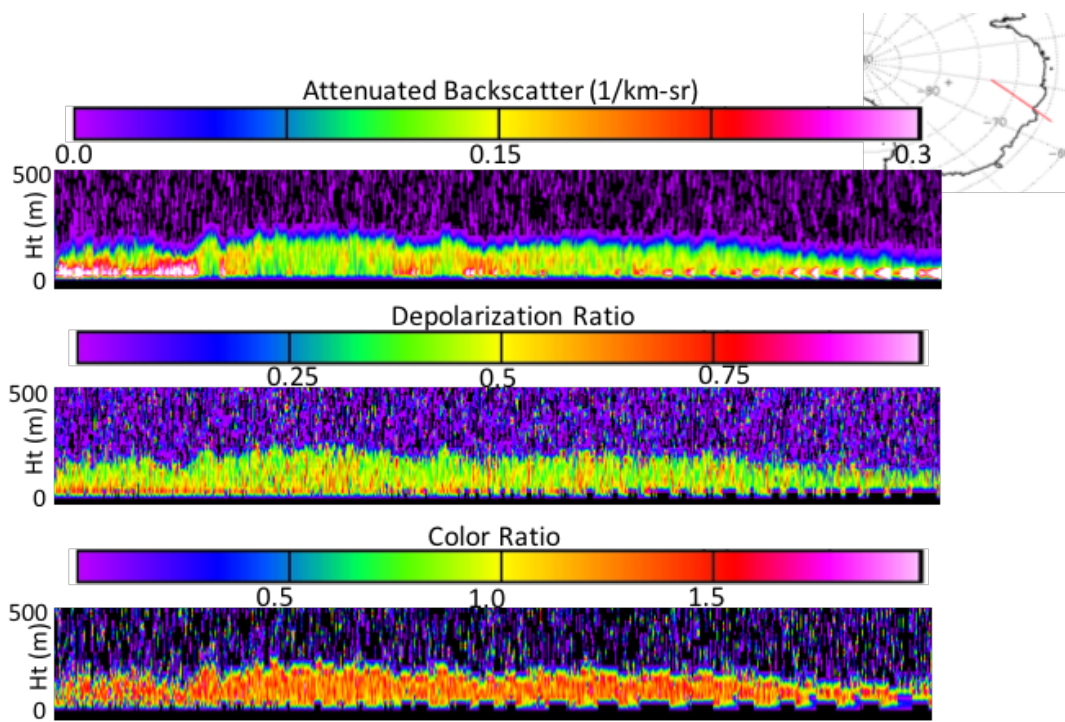
Year	Average Sublimation (mm swe)	Integrated Sublimation (Gt yr <sup>-1</sup> )
2006*	28.3	255
2007	56.8	514
2008	49.2	446
2009	45.3	409
2010	42.9	388
2011	47.6	431
2012	44.4	402
2013	47.7	432
2014	41.5	376
2015	41.3	374
2016*	33.2	301
<b>AVG</b>	<b>43.5*</b>	<b>393.4*</b>

643

644 Table II. The total transport (Gt yr<sup>-1</sup>) from continent to ocean for various regions in Antarctica  
 645 for 2007–2015.

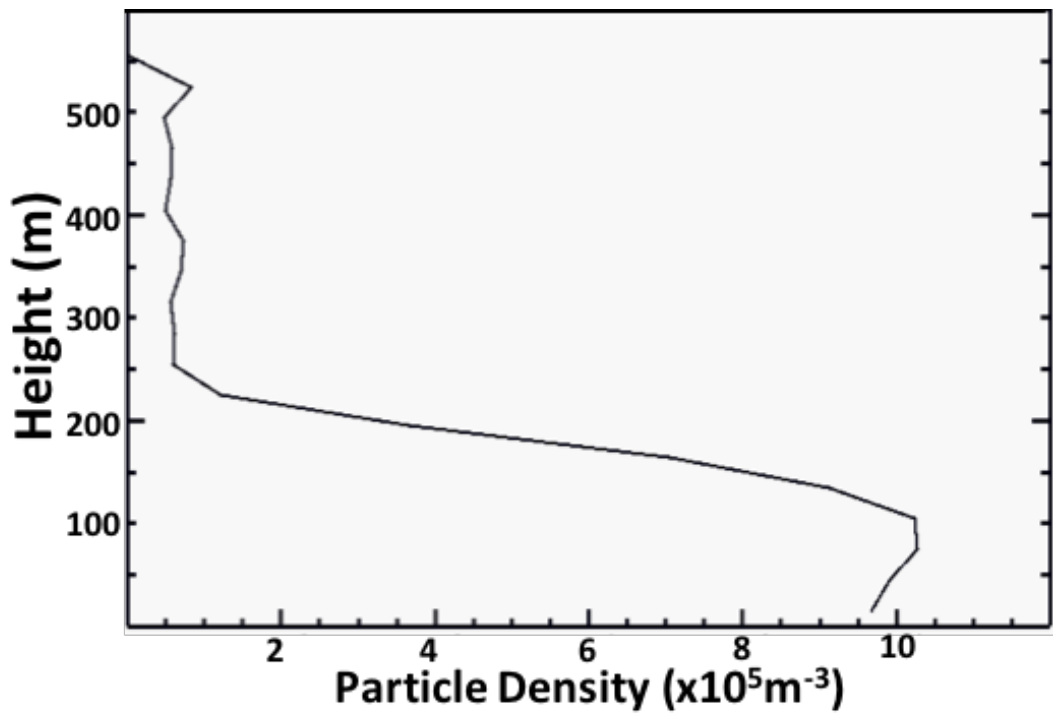
Year	East Antarctica	West Antarctica	135E – 160E	80W – 120W
2007	2.52	1.29	1.72	0.82
2008	2.20	1.43	1.21	0.90
2009	2.63	1.27	1.51	0.78
2010	2.26	1.15	1.38	0.73
2011	2.04	1.04	1.13	0.64
2012	2.49	1.21	1.41	0.73
2013	2.54	1.41	1.26	0.83
2014	2.55	1.02	1.49	0.67
2015	2.76	1.38	1.58	0.69
<b>Avg</b>	<b>2.44</b>	<b>1.24</b>	<b>1.41</b>	<b>0.75</b>

646



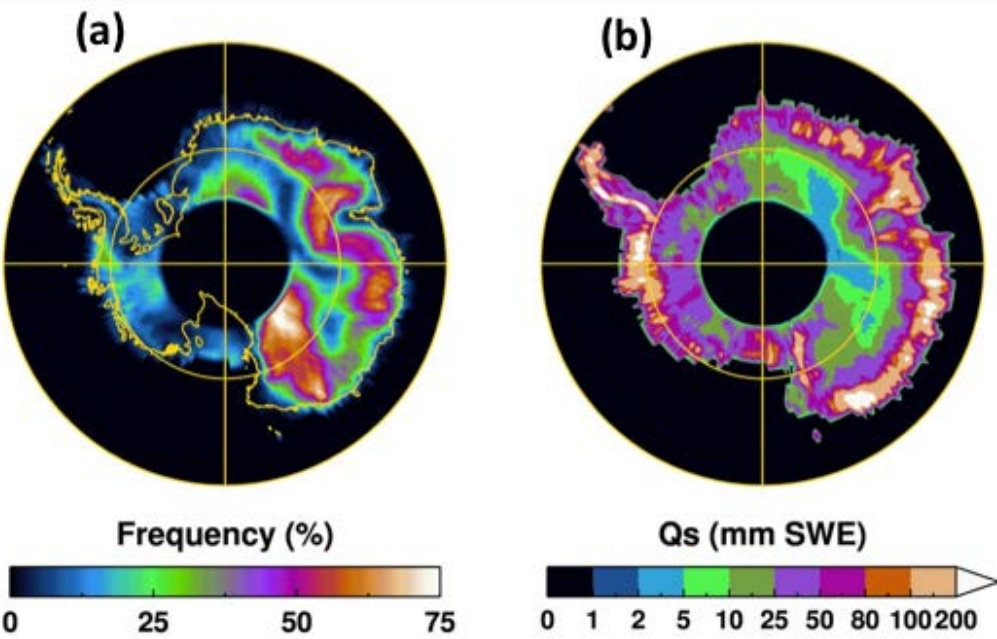
647

648 Figure 1. A typical Antarctic blowing snow layer as measured by CALIPSO on May 28, 2015 at  
649 17:08:41 – 17:11:33 UTC. Displayed (from top to bottom) are the 532 nm calibrated, attenuated  
650 backscatter, the depolarization ratio at 532 nm, and the color ratio (1064 nm / 532 nm).



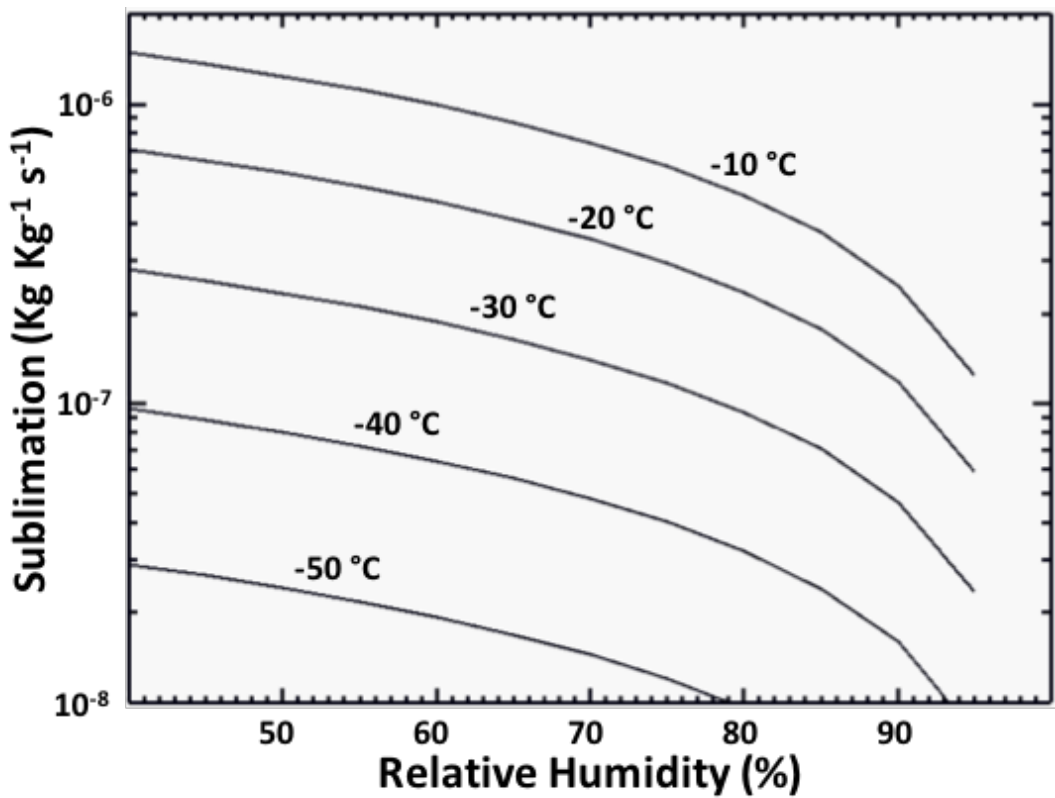
651

652 Figure 2. Average particle density profile (Eq. 2) through the blowing snow layer shown in Fig. 1.



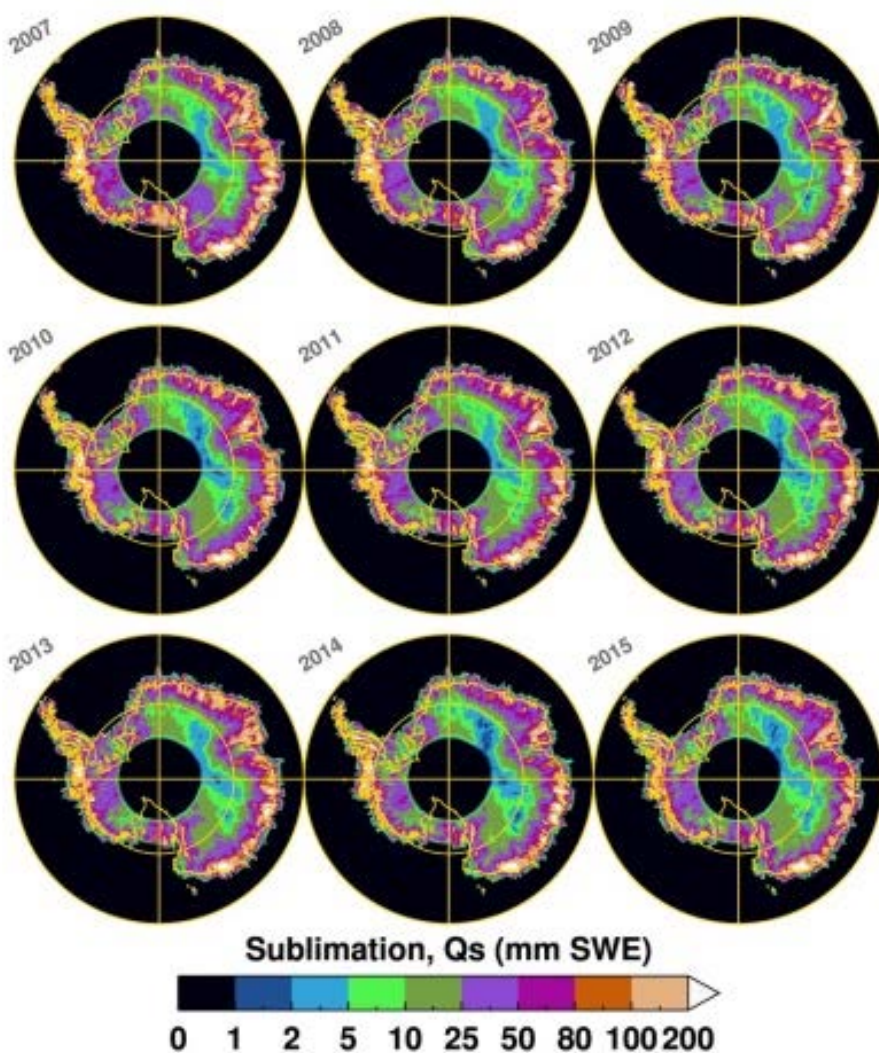
653

654 Figure 3. (a) The average April through October blowing snow frequency for the period 2007–  
655 2015. (b) The average annual blowing snow sublimation for the same period as in (a).



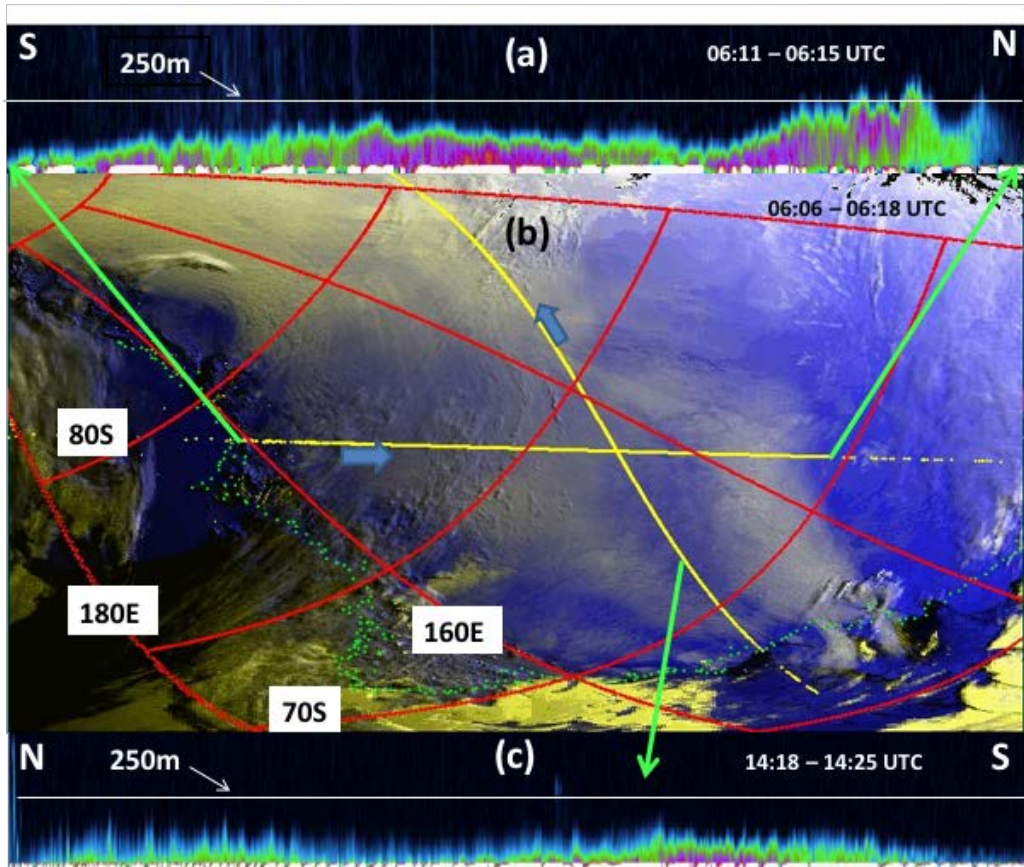
656

657 Figure 4. Computed blowing snow sublimation rate using Eqs. (3) and (4) as function of relative  
658 humidity for varying air temperatures. The particle density value used in Eq. (3) was 106 m<sup>-3</sup>  
659 which corresponds to a blowing snow mixing ratio ( $q_b$ ) of 4.7x10<sup>-5</sup> Kg Kg<sup>-1</sup>



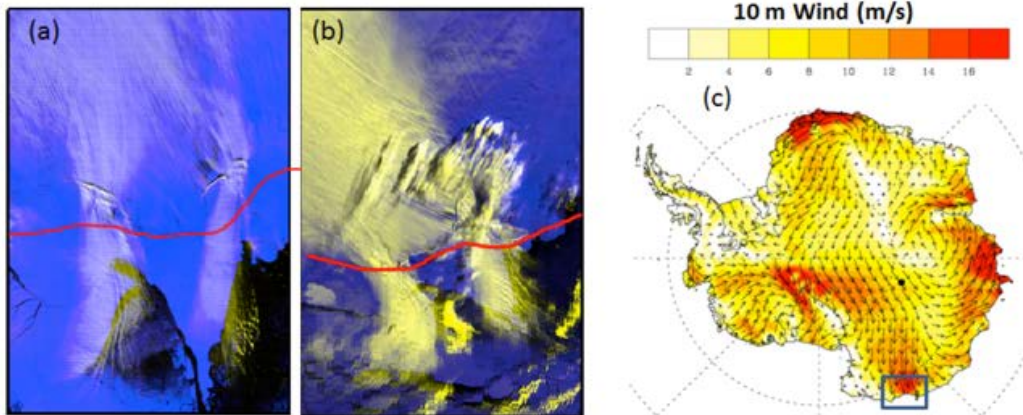
660

661 Figure 5. Blowing snow total sublimation over Antarctica by year for 2007–2015.



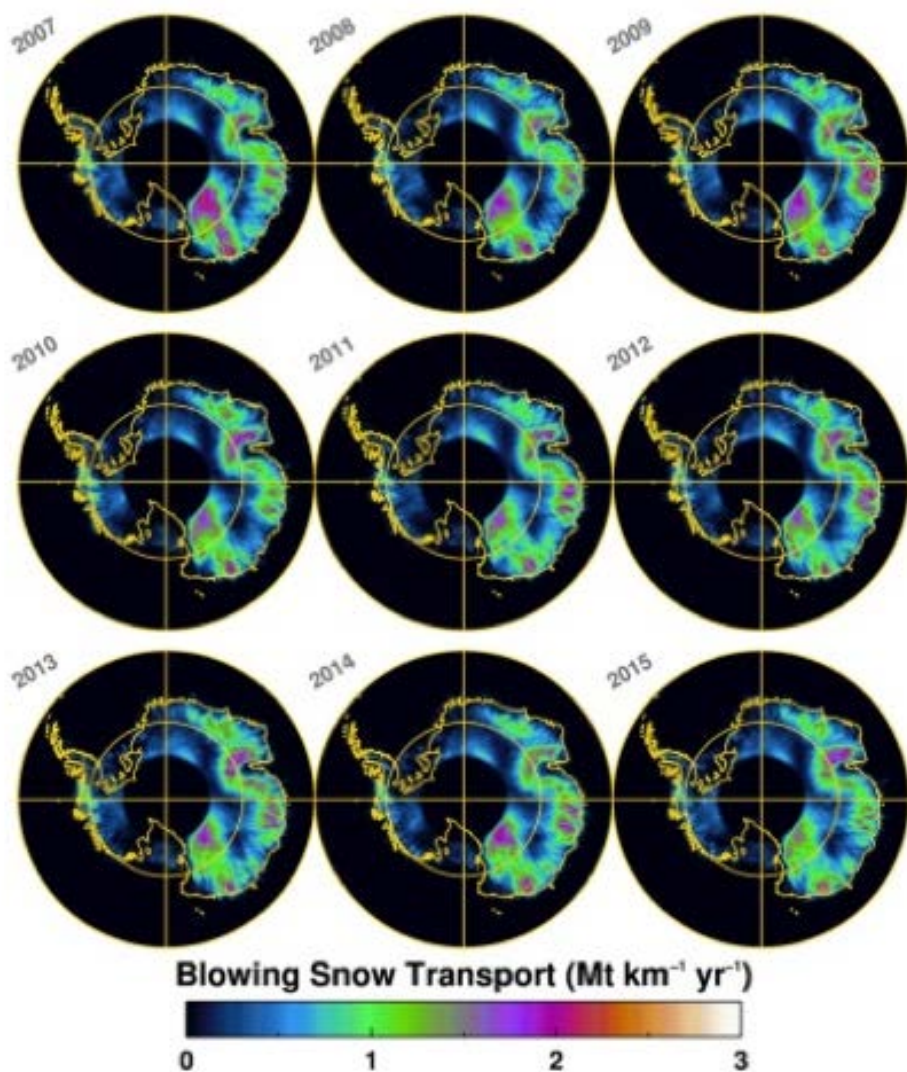
662

663 Figure 6. A large blowing snow storm over Antarctica with blowing snow transport from  
664 continent to ocean on October 14, 2009. (a) CALIOP 532 nm attenuated backscatter along the  
665 yellow (south to north) line bounded by the green arrows as shown in (b) at 06:11 – 06:15 UTC.  
666 (b) MODIS false color image at 06:06:14 – 06:17:31 UTC showing blowing snow as dirty white  
667 areas. The coastline is indicated by the green dots, and two CALIPSO tracks, where blowing  
668 snow was detected are indicated by the yellow lines. (c) CALIOP 532 nm attenuated backscatter  
669 along the yellow (north to south) line, 14:18 – 14:25 UTC.



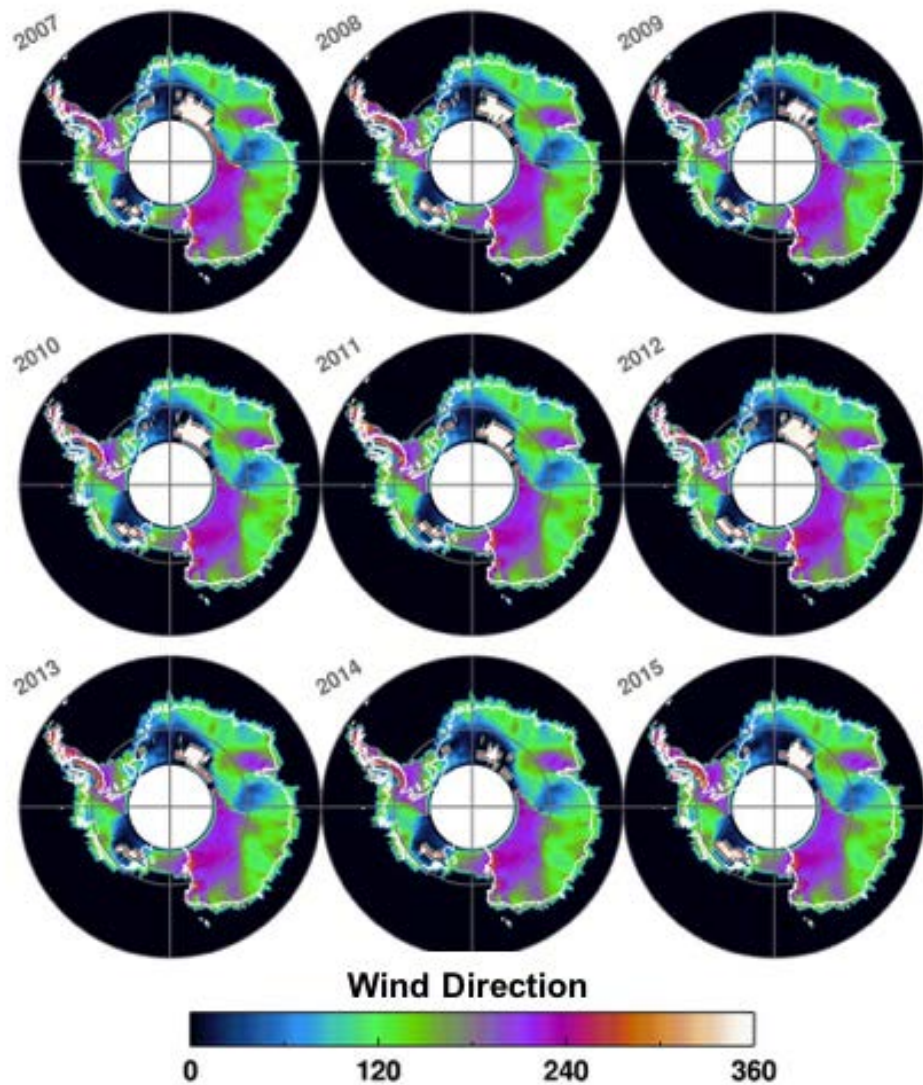
670

671 Figure 7. (a) MODIS false color image on October 13, 2009, 23:00 UTC and (b) October 14,  
672 2009, 06:16 UTC. The red line is the approximate position of the coastline. (c) The 10 m wind  
673 speed from the AMPS model (Antarctic Mesoscale Prediction System) for October 14, 2009. The  
674 area covered by the MODIS images is roughly that indicated by the blue box in (c).



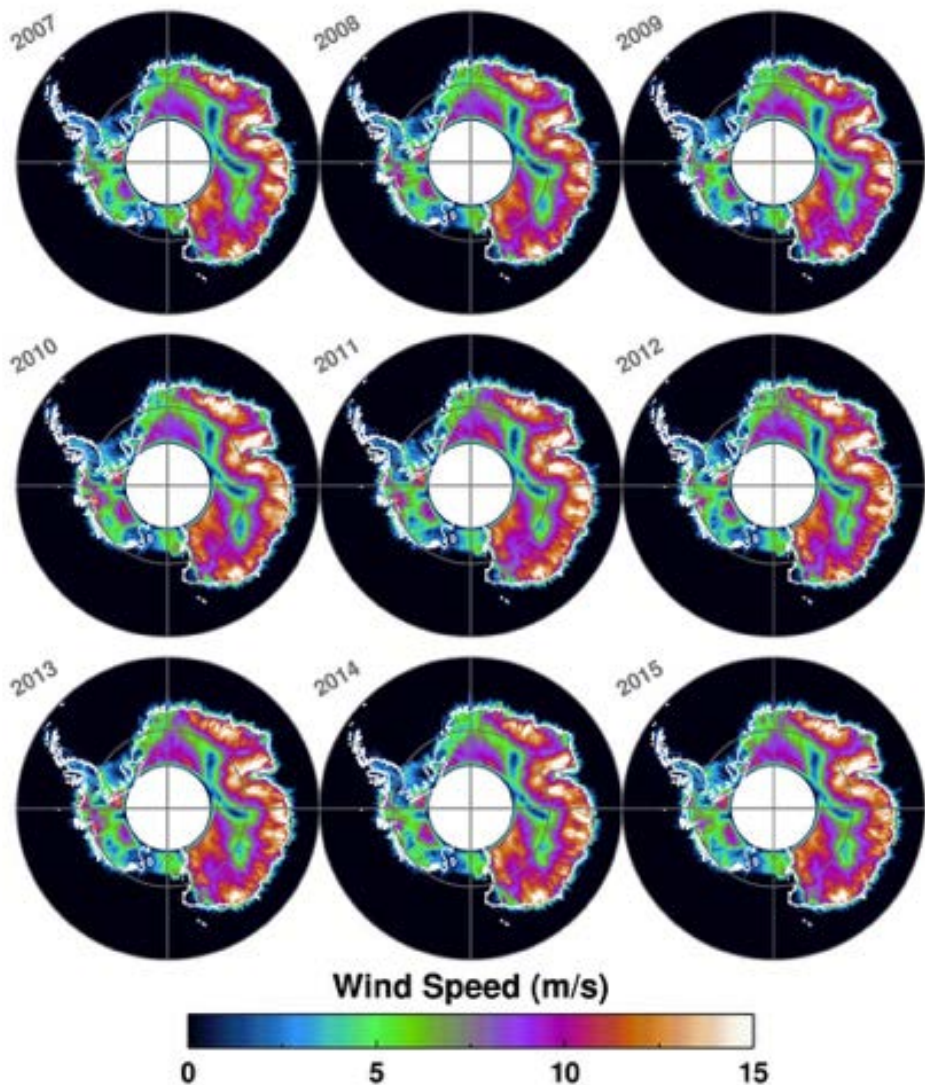
675

676 Figure 8. The magnitude of blowing snow transport over Antarctica integrated over the year for  
677 years 2007–2015.



678

679 Figure 9. The average wind direction over Antarctica for years 2007–2015



680

681 Figure 10. The average wind speed over Antarctica for years 2007–2015